DOI:10.1190/1.9781560801689.fm

3D Seismic Imaging

Biondo L. Biondi

Investigations in Geophysics Series No. 14

Michael R. Cooper, series editor

Gerry Gardner, volume editor

SOCIETY OF EXPLORATION GEOPHYSICISTS

Tulsa, Oklahoma, U.S.A.

DOI:10.1190/1.9781560801689.fm

ISBN 0-931830-46-X
ISBN 1-56080-137-9

Society of Exploration Geophysicists
P. O. Box 702740
Tulsa, OK 74170-2740

Published 2006
Printed in the United States of America

Library of Congress Cataloging-in-Publication Data
Biondi, Biondo, 1959-
3D seismic imaging / Biondo L. Biondi.
p. cm. -- (Investigations in geophysics ; no. 14)
Includes bibliographical references and index.
ISBN 0-931830-46-X -- ISBN 1-56080-137-9
1. Three-dimensional imaging. 2. Seismic reflection method. I. Title. II. Title: Three dimensional seismic imaging.
QE538.5.B56 2006 2006050641
551.0285'6693--dc22 CIP

To my parents

DOI:10.1190/1.9781560801689.fm

Table of Contents

DOI:10.1190/1.9781560801689.fm

DOI:10.1190/1.9781560801689.fm

About the Author

Biondo Biondi is associate professor (research) of geophysics at Stanford University in California. He is codirector of the Stanford Exploration Project (SEP) and leads its efforts in 3D seismic imaging. SEP is an academic consortium whose mission is to develop innovative seismic-imaging methodologies and to educate the next generation of leaders in exploration seismology. Biondi has made contributions in several aspects of seismic imaging, ranging from velocity estimation to parallel algorithms for seismic migration. Since the early 1990s, he has been at the forefront of the development of wave-equation 3D prestack imaging methods. In 1994, Biondo cofounded 3DGeo Development, a seismic-services company for practical applications of seismic imaging. It brings innovative technologies to the exploration industry, such as wave-equation imaging and Internet-based seismic processing.

Biondi graduated from Politecnico di Milano in 1984 and received an M.S. (1988) and a Ph.D. (1990) in geophysics from Stanford. He is a member of the Society of Exploration Geophysicists, the European Association of Geoscientists and Engineers, and the American Geophysical Union. In 2004, SEG honored him with its Reginald Fessenden Award for his development of azimuthal moveout.

DOI:10.1190/1.9781560801689.fm

Preface

In the past decade, 3D reflection seismology has replaced 2D seismology almost entirely in the seismic industry. Recording 3D surveys has become the norm instead of the exception. The application of 2D seismology is limited mostly to reconnaissance surveys or to locations where recording 3D data is still prohibitively expensive, such as in rough mountains and wild forests. However, academic research and teaching have struggled to keep up with the 3D revolution. As a consequence of this tardiness, no books are available that introduce the theory of seismic imaging from the 3D perspective. This book is aimed at filling the gap.

Seismic processing of 3D data is inherently different from 2D processing. The differences begin with data acquisition: 3D data geometries are considerably more irregular than 2D geometries. Furthermore, 3D acquisition geometries are never complete because sources and receivers are never laid out in dense areal arrays covering the surface above the target. These fundamental differences, along with the increased dimensionality of the problem, strongly influence the methods applied to process, visualize, and interpret the final images. Most 3D imaging methods and algorithms cannot be derived from their 2D equivalent by merely adding a couple of dimensions to the 2D equations. This book introduces seismic imaging from the 3D perspective, starting from a 3D earth model. However, because the reader is likely to be familiar with 2D processing methods, I discuss the connections between 3D algorithms and the corresponding 2D algorithms whenever useful.

The book covers all the important aspects of 3D imaging. It links the migration methods with data acquisition and velocity estimation, because they are inextricably intertwined in practice. Data geometries strongly influence the choice of 3D imaging methods. At the beginning of the book, I present the most common acquisition geometries, and I continue to discuss the relationships between imaging methods and acquisition geometries throughout the text. The imaging algorithms are introduced assuming regular and adequate sampling. However, Chapters 8 and 9 explicitly discuss the problems and solutions related to irregular and inadequate spatial sampling of the data.

Velocity estimation is an integral component of the imaging process. On one hand, we need to provide a good velocity function to the migration process to create a good image. On the other hand, velocity is estimated in complex areas by iterative migration and velocity updating. Migration methods are presented first in the book because they provide the basic understanding necessary to discuss the velocity updating process.

Seismic-imaging algorithms can be divided into two broad categories, integral methods (e.g., Kirchhoff methods) and wavefield-continuation methods. Integral methods can be described by simple geometric objects such as rays and summation surfaces. Thus, they are understood more easily by intuition than wavefield-continuation methods are. My introduction of the basic principles of 3D imaging exploits the didactic advantages of integral methods. However, wavefield-continuation methods can yield more accurate images of complex subsurface structures. This book introduces wavefield-continuation imaging methods by leveraging the intuitive understanding gained during the study of integral methods. Wavefield-continuation methods are the subject of my ongoing research and that of my graduate students. Therefore, the wavefield-continuation methods described are more advanced, although less well established, than the corresponding integral methods.

Seismic-imaging technology is data driven, and the book contains many examples of applications. The examples illustrate the rationale of the methods and expose their strengths and weaknesses. The data examples are drawn both from real data sets and from a realistic synthetic data set, the SEG-EAGE salt data set, which is distributed freely and used widely in the geophysical community. For the reader's convenience, a subset of this data set (known as C3 narrow-azimuth) is contained in the DVD included with this book. Appendix 2 briefly describes this data set.

The software needed to produce many examples also will be distributed freely over the Internet. A reader with the necessary computer equipment (a powerful Unix workstation) and the patience to wait for weeks-long runs could reproduce the images obtained from the SEG-EAGE salt data

set. Appendix A describes the foundations of SEPlib3d, the main software package needed to generate most of the results shown in this text.

The book starts from the introduction of the basic concepts and methods in 3D seismic imaging. To follow the first part of the book, the reader is expected to have only an elementary understanding of 2D seismic methods. The book thus can be used for teaching a first-level graduate class as well as a short course for professionals. The second part of the book covers more complex topics and recent research advances. This material can be used in an advanced graduate class in seismic imaging. To facilitate the teaching of the material in this book, the attached DVD includes a document in PDF format that has been formatted specifically to be projected electronically during a lecture. All the figures in this electronic document can be animated by clicking on a button in the figure caption. Several of these figures are movies that provide a more cogent illustration of the concepts described in the text. All figures are included on the attached DVD as GIF files.

DOI:10.1190/1.9781560801689.fm

Acknowledgments

This book benefits endlessly from the contributions of faculty and students at the Stanford Exploration Project (SEP), Stanford University. Jon Claerbout, the inspiring founder of SEP, has influenced every aspect of my work. I am particularly grateful to him for demonstrating how much fun and how insightful the exploration of real seismic data can be. This book would be much poorer in data examples without his influence.

All the data examples have been produced using the SEPlib software library, particularly its 3D extension named SEPlib3D. SEPlib and its related graphic software were built and refined by several generations of SEP students. Jon Claerbout and Stew Levin started SEPlib itself. Rob Clayton, Dave Hale, Joe Dellinger, and Rick Ottolini developed most of the graphic software. Their work was continued by Dave Nichols and Steve Cole. SEPlib3d owes its existence to Bob Clapp. He and I collaborated in SEPlib3d design and initial implementation, which was based on early work by Martin Karrenbach. Clapp deserves all the credit if SEPlib3d is now an excellent tool for 3D seismic research, still unmatched in its flexibility and capabilities.

I have been working on this book for several years, and I used it as a textbook for my yearly course on 3D seismic imaging at Stanford. Students of this class have provided innumerable and original suggestions that helped make the text clearer and more readable. Several figures have been produced by SEP students. I acknowledge these important contributions in the captions of the relevant figures.

Gerry Gardner kindly agreed to be the SEG volume editor for this book. He has been very patient during the several years that I took to complete the manuscript and has given me many invaluable suggestions. His pioneering work in 3D imaging is at the basis of many of the methods presented in my book.

I am also grateful to professional geophysicists who read early versions of the book as I posted them on the Web and have contributed to the correction of several errors in the text and in equations. Among them, Bill Schneider and Zheng-Zheng (Joe) Zhou have been particularly helpful. Dawn Burgess and Fannie Gray, SEP technical editors, carefully edited the manuscript and patiently expunged the Latinisms in my English writing. Anne Thomas, who copy edited the book for SEG, did a great job of getting the manuscript into its final form.

I thank my publisher, SEG, and especially the following staff members: Rowena Mills (manager of GEOPHYSICS and books) for patiently driving the process of making a published book out of a LaTex manuscript and for the final proofreading, along with editorial coordinator Julie Colley; William D. Underwood for helping the proofreading process when geophysical issues surfaced; and Ted Bakamjian (director of publications) for his support.

I also thank Michael R. Cooper (SEG's Investigation in Geophysics Series editor) for persistently cajoling me to stop adding material to the manuscript and finally submit it to SEG.

My research is supported financially by the sponsors of SEP. I am grateful to all of them for making the writing of this book possible. Several of those companies and a few other organizations have provided the real data sets used in data examples. I would like to thank the following people and organizations (in alphabetical order) for providing the data sets used in this book: BP (ARCO) for the buttonpatch data geometry used in Chapter 1; Frederic Billette and John Etgen, along with BP and ExxonMobil, for the deepwater Gulf of Mexico data set used in Chapters 9 and 12; Bob Brown and Chevron for the Gulf of Mexico data set used in the introduction; John Toldi and Chevron for the OBC data geometry used in Chapter 1; Doug Hanson with ConocoPhillips and ExxonMobil for the North Sea data set used in the introduction, Chapters 3 and 9, and Appendix A; Trino Salinas and Ecopetrol for the South America data set used in Chapter 9; Husky Oil for the cross-swath data geometry used in Chapter 1; IFP for the Marmousi data set used in Chapter 8; Bill Symes and the TRIP project at Rice University for the synthetic data set used in Chapters 4 and 6; SEG and EAGE for the salt data set used throughout the book; Josef Paffenholz (now with Fairfield Industries) and the SMART JV for the Sigsbee data set used in Chapters 9 and 12; Henri Calandra and Total for the North Sea data set

used in Chapters 7, 9, and 11; Wook Lee (now with SeisLink Corporation) and Unocal for the Gulf of Mexico OBC data set used in the introduction and Chapters 5 and 8; Phil Schultz and Unocal for the deepwater Gulf of Mexico data set used in Chapter 7. The images of this data set shown in Chapter 7 were produced by Sean Crawley and Moritz Fliedner (with 3DGeo) and were kindly provided by 3DGeo Development.

Introduction

The driving force behind the fast switch from 2D seismology to 3D seismology is the dramatic increase in information and accuracy that 3D seismic images yield, compared with images obtained by 2D seismic. That increase is substantial not only for structures that are obviously three-dimensional, such as the Gulf of Mexico salt dome shown in Figures 1 and 2, but also for areas where the geology has a predominant dip direction, such as the North Sea data shown later in this introduction. Furthermore, at the reservoir scale, the earth is seldom two-dimensional. Only 3D imaging can provide the detailed knowledge of small-scale reservoir features, such as small faulting and thin channeling. This knowledge often is crucial to an effective exploration and production strategy. We will see in an upcoming figure an example of a complex channel system that would have been undetected without 3D seismic data.

The economic value provided by the quality and quantity of available information is compounded with a substantial reduction in costs related to 3D seismic acquisition and processing. This technological trend is continuing unabated, and it is likely to continue for the foreseeable future, as 3D seismic data acquisition and processing become more widespread and achieve even larger economies of scale.

In this introduction, we will explore the differences between images obtained from 2D seismology and from 3D seismology, and we will gain an understanding of the causes of these differences and of the new challenges presented by 3D seismic imaging.

2D versus 3D seismology: More accurate imaging

Improvements assured by 3D seismology over 2D seismology in imaging the subsurface are well illustrated by the images shown in Figures 1 and 2. The figures compare the results of applying 3D and 2D poststack depth migration to a zero-offset cube (Chapter 2). The sections on the left show the results of full 3D migrations of the data; the sections on the right show the results of performing independent 2D migrations on each inline section (horizontal direction in Figure 1b). If we had available only 2D data collected along any of the inlines, we would have obtained the distorted images of the subsurface corresponding to the inline sections extracted from the 2D migrated cube (e.g., Figure 2b). The depth slices shown in Figure 1 show how the shape and extent of the salt dome would have been grossly misinterpreted from 2D images (Figure 1b). If the only image available were the 2D inline section shown in Figure 2b, the interpreter would have positioned a salt dome below the subsurface at a location where only sediments are present in reality (Figure 2a).

When we acquire a 2D seismic survey, we assume implicitly that the earth is a cylinder, with its axis in the direction orthogonal to the survey. If this underlying assumption is fulfilled, the image obtained by 2D seismic interpretation is an accurate representation of a vertical section of the subsurface. However, when this assumption is not fulfilled, 2D seismic interpretation produces a distorted image of the subsurface. The schematic in Figure 3 shows the main reasons why 2D seismic interpretation produces distorted images when we are imaging 3D structures. The point diffractor R_{3D} is out of the plane with respect to the 2D acquisition direction. It creates reflections that are incorrectly back-propagated in the earth along the vertical plane passing through the acquisition direction and that are imaged at the wrong location R_{2D}. To image the diffractor at its correct location R_{3D}, we need to apply 3D imaging for back-propagating the recorded reflection along an oblique plane. However, even after applying 3D imaging methods to a single 2D line, we would be left with the ambiguity of where to place the diffractor along the semicircular curve perpendicular to the acquisition direction, marked as *Crossline migration* in the figure.

To resolve this ambiguity, we estimate the crossline component of the propagation direction. This estimate is possible only by measuring the reflection stepout along the crossline direction — that is, by recording 3D data. Figures 4 and 5 schematically illustrate this concept. Seismic imaging algorithms rely on the difference in the arrival times of the same event recorded by nearby traces (time stepout) to estimate the direction of event propagation. The nearby traces may correspond to different receiver locations (G in the figures) or to different source locations (S in the figures).

This estimate usually is implicit in the imaging algorithms, but nevertheless, it is crucial to the imaging process. If data are recorded along only one direction (Figure 4), the only information available is about the angle that the propagation direction makes with the recording direction. No information is available on the crossline angle. Conversely, if data are recorded along both horizontal directions (Figure 5), the propagation direction can be resolved fully. Notice that at least in principle, for the imaging problem to be fully determined, the wavefield needs to be sampled properly at both the source and receiver locations. Unfortunately, that is rarely the case with practical acquisition geometries.

When 2D imaging is performed, the error in positioning the diffractor has both a crossline direction component Δy and a depth component Δz. The reflector R_{2D} needs to be moved along a semicircle in the crossline direction to be placed at its correct position R_{3D}. In the following, we will see that at least when the velocity is constant, this semicircular trajectory corresponds to the semicircle of a zero-offset crossline migration. The analytical expression

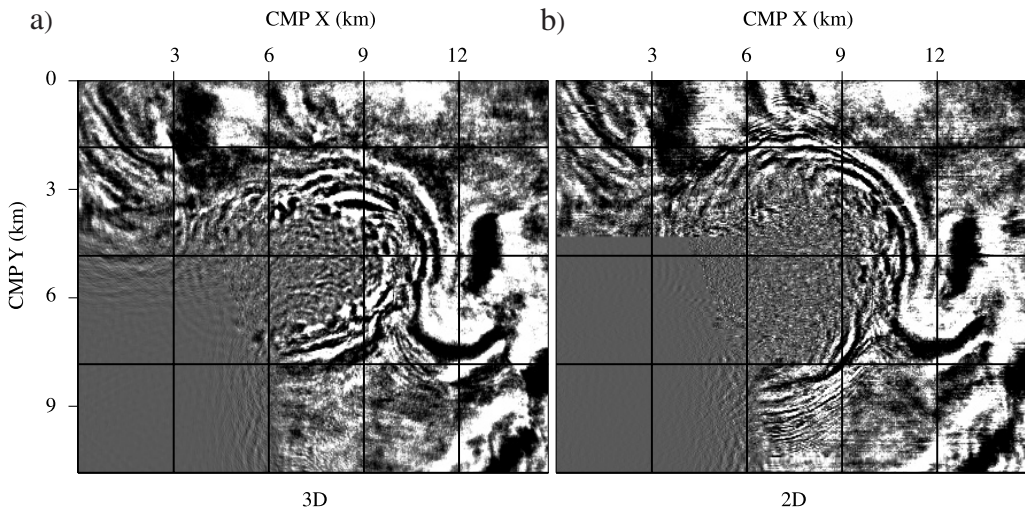

Figure 1. Depth slices of a Gulf of Mexico salt dome: (a) 3D versus (b) 2D. The slice is cut at depth = 3.63 km.

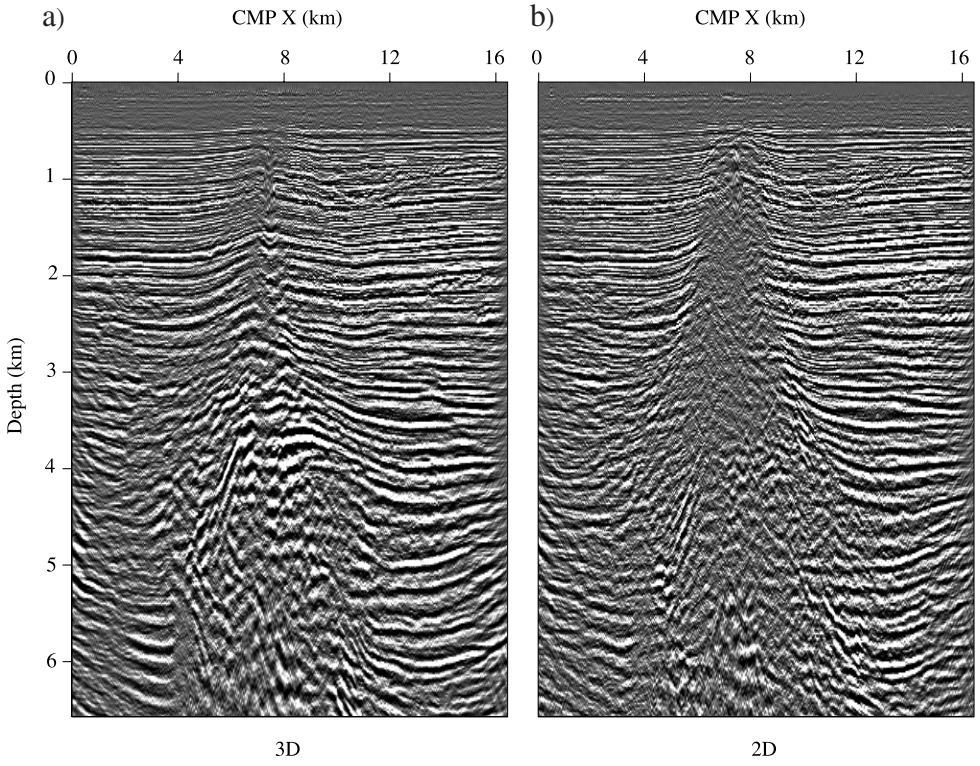

Figure 2. Inline sections of a Gulf of Mexico salt dome: (a) 3D versus (b) 2D. The section is cut at CMP Y = 3.25 km.

of this semicircle is independent of velocity and depends only on the apparent depth ρ of the reflector; that is,

$$\Delta y^2 + (\rho - \Delta z)^2 = \rho^2. \quad (1)$$

In this simple case, therefore, the imaging of 3D data can be performed as two sequential steps: (1) imaging along 2D lines, followed by (2) crossline migration. However, when the propagation velocity is not constant, this simple decomposition of 3D imaging is not correct, and full 3D migration is required. In the general case, the inline 2D migration cannot focus all the data properly because the velocity function V_{2D} along the vertical plane is different from the true velocity function V_{3D} along the oblique plane. When velocity variations are large, the propagation paths do not even lie on planes; they lie along more complex surfaces.

The next several figures show concrete examples of the different types of error introduced by 2D imaging when it is applied to geologic structures that present 3D features. The figures compare the sections of prestack depth-migrated cubes. The (a) sections on the left show the results of full 3D migrations of the data; the (b) sections on the right show the results of performing independent 2D migrations on parallel seismic lines. Figure 6 shows, in a crossline section, the mispositioning of reflectors caused by 2D imaging. The arrows point to two dipping reflectors that are grossly mispositioned by 2D imaging. From the 2D image, the width of the channel between the two reflectors would be underestimated by about 300 m. Figure 7 shows the need for a crossline migration to focus the data properly. The diffractions created by a rough salt-sediment interface, indicated by the arrows in the figure, are correctly collapsed only in the 3D image.

The errors in the structural interpretation caused by 2D seismic are illustrated further in Figure 8. This figure shows depth slices that cut through the same 2D-imaged and 3D-imaged cubes as in the previous figures. The broad reflection indicated by arrow B has been mispositioned by several hundred meters, but even more evident are the misfocusing and mispositioning of the reflector indicated by arrow A. The results of 2D imaging show a bowtie shape instead of the correct sinusoidal shape.

The lack of proper crossline migration is not the only cause for inaccurate structural imaging by 2D seismic acquisition and processing in a 3D world. When propagation velocity varies significantly in the crossline direction, the velocity function (V_{2D}) that is used to back-propagate the reflections along the vertical plane is generally different from the correct velocity function (V_{3D}) that should be used for propagating the reflections along the correct oblique plane. Use of a wrong velocity function causes both a mispositioning and a defocusing of the imaged reflectors. By comparing two inline sections from the image cubes previ-

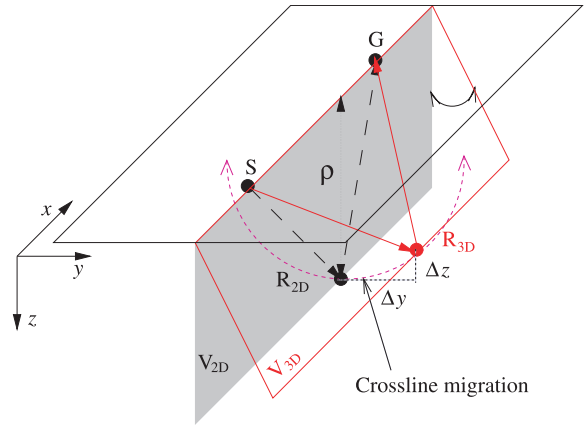

Figure 3. 2D versus 3D imaging of an out-of-plane diffractor.

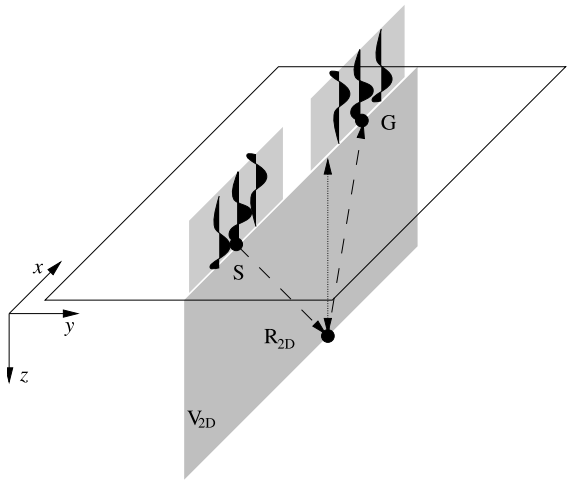

Figure 4. 2D acquisition and imaging. Only the in-plane propagation direction can be determined from 2D data.

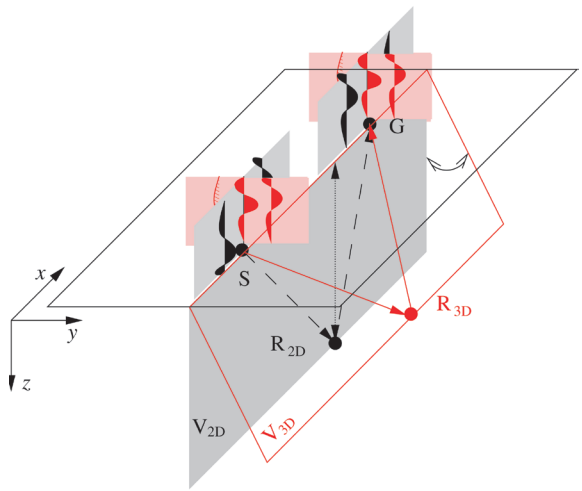

Figure 5. 3D acquisition and imaging. The data contained in the red traces allow the unambiguous determination of the propagation direction and positioning of the diffractor.

ously presented, Figure 9 shows an example of the misfocusing introduced by 2D seismology. The reflections from the salt flanks (Arrow A) and the reflections for the bottom of the salt (Arrow B) are significantly better focused in the 3D image than in the 2D image. Notice also the better focusing of the reservoir interval (Arrow C).

2D versus 3D seismology: Extra information

In the previous section, we saw examples of errors introduced by 2D imaging of 3D structures. Three-dimensional seismic information not only can increase the accuracy of structural images of the subsurface, it also provides a wealth of stratigraphic information that is not present in 2D seismic data.

Figure 10 shows an example of geologic information that would be impossible to recover from a set of 2D lines. The time slice in Figure 10a displays a complex channel system embedded in sediments in the proximity of a salt dome in the Gulf of Mexico. These channels are thin features, barely above the threshold of seismic resolution. If we had available only the inline section shown in Figure10b, it would be difficult even to detect the presence of the channels. It would be impossible to reconstruct the complex 3D structure of the channel system.

Even when the geologic structure is two-dimensional or one-dimensional, 3D seismic data can provide additional information on the rock's parameters. That additional information is contained in the data recorded along different source-receiver azimuthal directions. Typically, land data are acquired with a wide range of azimuthal directions, whereas marine data have a narrower range. However, even for marine data, the industry trend is toward acquiring surveys with a wider range of azimuths for the source-receiver pairs, both because of the widespread use of multistreamer acquisition configurations and because of the increasing use of ocean-bottom-cable (OBC) surveys. Recording data with a wide source-receiver azimuth provides additional information on subsurface properties. For example, measuring propagation velocity and reflectivity along different azimuthal directions can be useful in estimating anisotropic properties caused by vertical fracturing in reservoir rocks. The imaging methods described in this book assume an isotropic earth; therefore, they cannot be applied directly to imaging an anisotropic earth. However, the basic concepts of 3D imaging still are essential when one is extracting anisotropy information from 3D data. Tsvankin (2001) provides a good introduction to the issues related to anisotropic imaging.

The availability of high-resolution 3D images also has paved the way for time-lapse seismic data (Jack, 1997), which often is referred to as 4D seismic data. Time-lapse seismic data are used to monitor the evolution of a reservoir over time and to contribute to the development of optimal strategies for managing reservoirs. In this book, I do not focus on application of 3D imaging to 4D seismic data; nevertheless, the success of time-lapse studies depends on the quality of 3D imaging. Often, the changes over time in

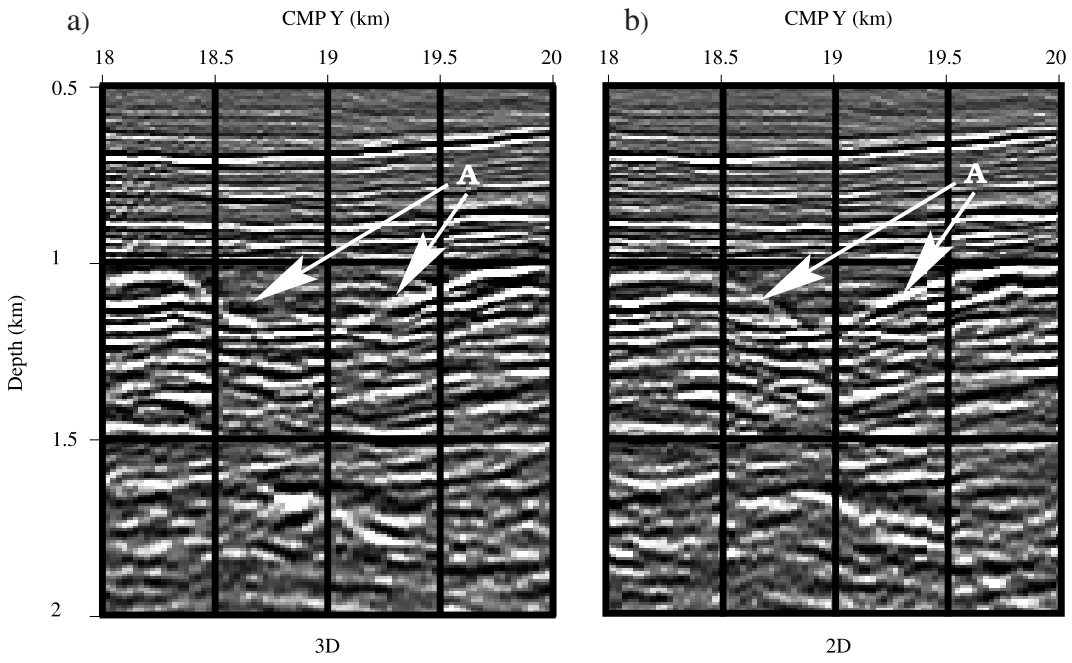

Figure 6. Crossline sections showing that 2D imaging causes lateral mispositioning of dipping reflectors.

a reservoir's seismic properties are small and close to the seismic resolution; only high-fidelity imaging can uncover them properly.

2D versus 3D seismology: New challenges

Many of the basic concepts that have been developed for 2D seismic imaging are still valid for 3D imaging. However, 3D imaging presents several new problems that are caused by the 3D data's higher dimensionality. As we will see in more detail in Chapter 1, 3D seismic prestack data are defined in a 5D space, compared with the 3D space of 2D prestack data. The five dimensions are the recording time (t), the two components of the source position (x_s, y_s), and the two components of the receiver position (x_g, y_g).

An obvious problem related to the high dimensionality of 3D seismic data is the amount of data that is recorded in the field and that needs to be processed. Modern surveys often produce several terabytes of data. Such large quanti-

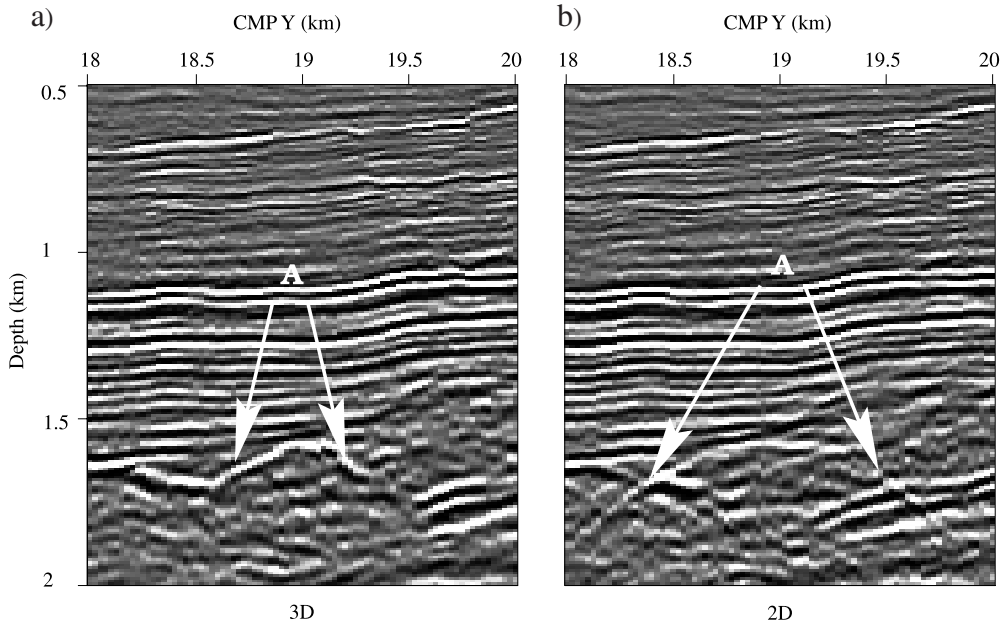

Figure 7. Crossline sections showing that 2D imaging does not focus diffractions properly.

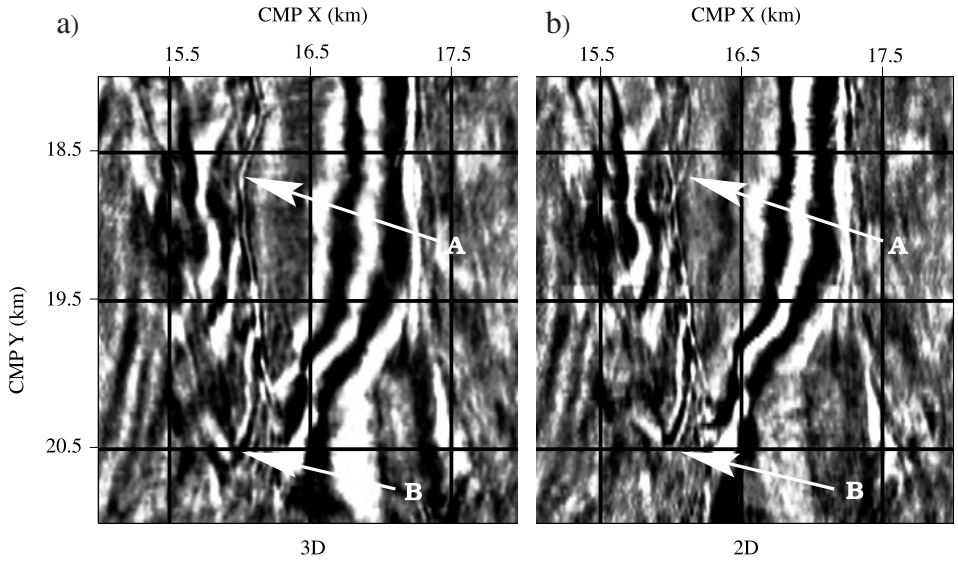

Figure 8. Depth slices showing that 2D imaging causes misfocusing and lateral mispositioning.

ties of data are difficult to handle, visualize, and process. An important aspect of processing a 3D data set is to devise the right strategy for reducing the time and resources necessary to obtain an image of the subsurface from the original large data set, without compromising the accuracy of the results.

The two most common methods for reducing processing cost are aimed at reducing the dimensionality of the computational domain. These methods are useful in 2D work, but they are essential in 3D work, because of the higher dimensionality of the data space. The first method, commonly called stacking, reduces the size of the data set by

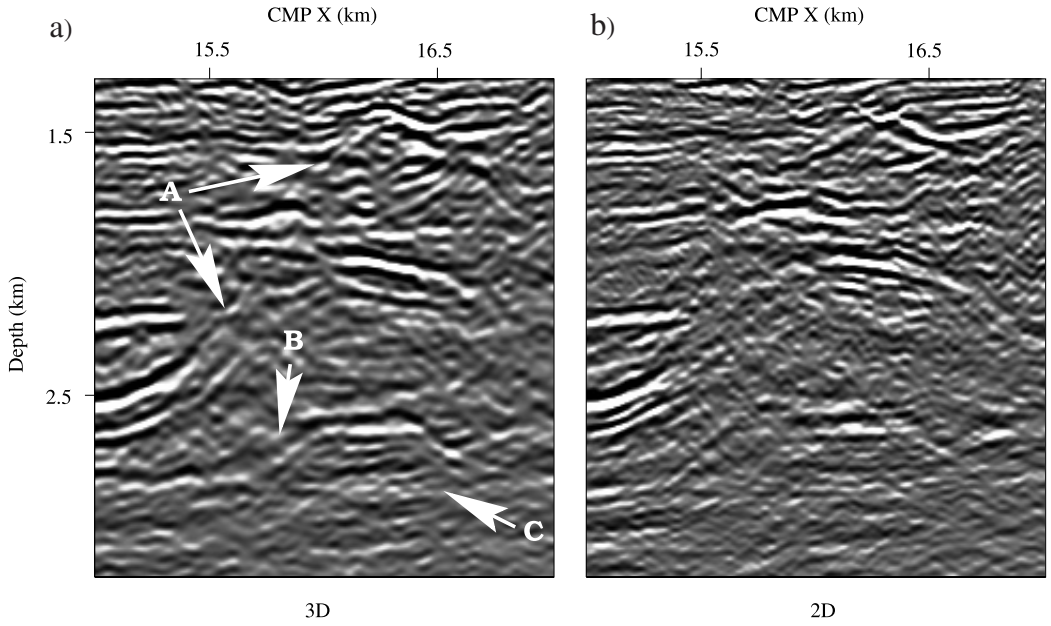

Figure 9. Inline sections showing that 2D images are misfocused because of lateral velocity variations.

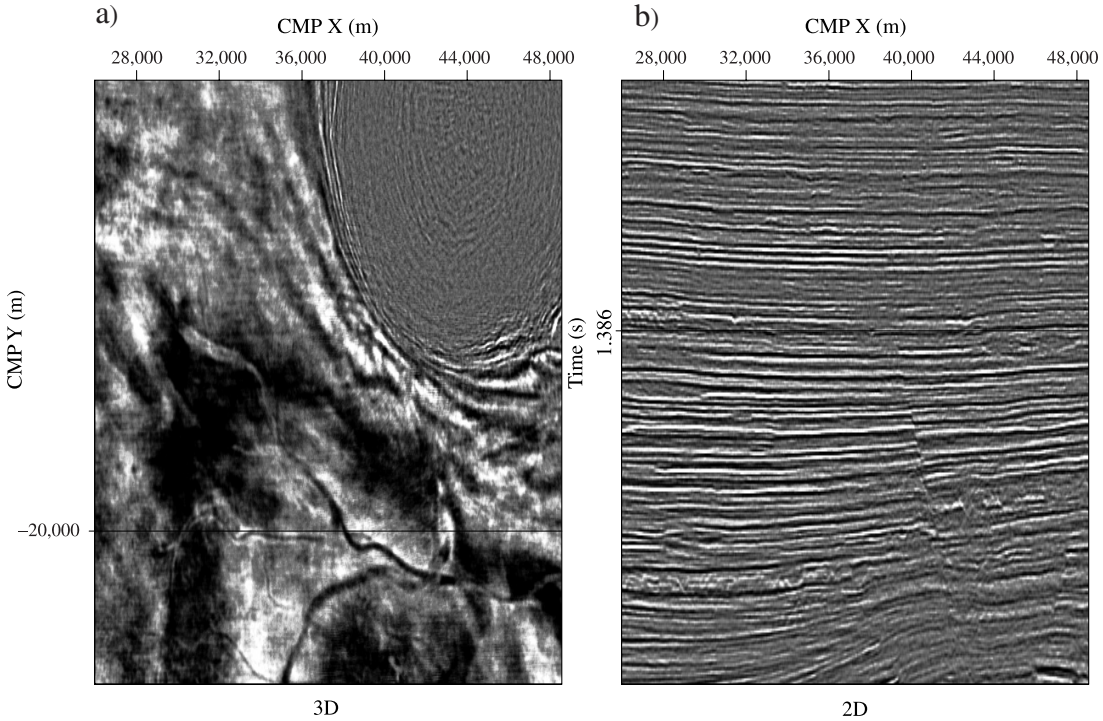

Figure 10. Time slice (t = 1.386 s) and inline section (CMP X = –20,000 m) of a 3D image from data recorded in the Gulf of Mexico. Notice the complex channel system is visible in the time slice in (a). It would be impossible to reconstruct that channel system from a set of vertical slices such as the section in (b).

averaging the recorded traces along appropriate ranges of the four spatial axes. The most common example of stacking is offset stacking, in which recorded traces are averaged over offset after the application of normal moveout (NMO) (Chapter 3). Offset stacking yields a great reduction in computational cost, because the cost of many imaging operators is directly proportional to the size of the input data. Common-azimuth migration (Chapter 7) is another example of an imaging algorithm that achieves high computational efficiency by exploiting a reduction in data dimensionality (from five dimensions to four dimensions). In this case, a common-azimuth data set is generated from marine data that are averaged over azimuths after applying azimuth moveout (AMO) (Chapter 3). Common-azimuth data are then imaged by using a wavefield-continuation migration method.

The second methodology used to reduce computational complexity is based on full separation, or splitting, of the computations along different data axes. Two-pass migrations are typical examples of applications of full-separation methods. In general, by decoupling the computations along an axis x of length n_x and an axis y of length n_y, we reduce the computational cost from being of order $O(n_x \times n_y)$ to being of order $O(n_x + n_y)$. The cost advantages of stacking and of separation are achieved at the expense of generality; the derived imaging methods are accurate only for particular classes of data sets. Because selection of the appropriate processing strategy is a crucial decision, we will discuss the available choices as a function of their trade-offs between accuracy and speed.

The other major challenge of 3D seismic data collection and processing is that 3D prestack seismic data are sampled sparsely and irregularly along the spatial coordinates (x_s, y_s, x_g, y_g). Because of practical and economic considerations, actual 3D surveys recorded in the field (Chapter 1) never record seismic traces at every possible location for the source and the receiver, and therefore the data never fill the 5D space potentially available. On the contrary, much effort is spent to optimize survey design so that the desired accuracy in the image is achieved and the number of recorded traces is minimized. The result is that the seismic wavefield almost never is well sampled along both the source axes and the receiver axes. The condition for unambiguous imaging that we introduced in the discussion of Figure 5 thus is seldom fulfilled. To generate high-fidelity images, we must safeguard our imaging algorithm from generating aliasing artifacts (Chapter 8). Crucial to this goal is exploiting the redundant information contained in the recorded data by making assumptions on both the reflectivity model and the complexity of the wave propagation.

Irregularity in spatial sampling may cause severe variation in the spatial illumination of the subsurface. Depending on the degree of variability in data density and the complexity of the imaging algorithm, irregular sampling may cause distortions in the image amplitudes and it may create coherent artifacts in the image. Chapter 9 introduces the basic concepts for compensating for variable data density by normalizing imaging operators. It also introduces a method that exploits data redundancy to reduce both aliasing and irregular sampling artifacts.

References

Jack, I. G., 1997, Time-lapse seismic in reservoir management: Society of Exploration Geophysicists.

Tsvankin, I., 2001, Seismic signatures and analysis of reflection data in anisotropic media: Elsevier Science.

DOI:10.1190/1.9781560801689.fm